Since January 2020 Elsevier has created a COVID-19 resource centre with free information in English and Mandarin on the novel coronavirus COVID-19. The COVID-19 resource centre is hosted on Elsevier Connect, the company's public news and information website.

Sustainable Cities and Society 85 (2022) 104061

Contents lists available at ScienceDirect

Sustainable Cities and Society

journal homepage: www.elsevier.com/locate/scs

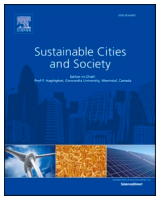

New sights on the impact of spatial composition of production factors for socioeconomic recovery in the post-epidemic era: a case study of cities in central and eastern China

Shidong LIU [a,b,#], Jie ZHANG [c,#], Jianjun ZHANG [a,d,*]

[a] School of Land Science and Technology, China University of Geosciences (Beijing), Beijing 100083, China
[b] Faculty of Science, University of Copenhagen. Copenhagen 1350, Denmark
[c] Institute of Geographic Sciences and Natural Resources Research, CAS, Beijing 100101, China
[d] Key Laboratory of Land Consolidation and Rehabilitation, Ministry of Natural Resources, Beijing 100083, China

ARTICLE INFO

Keywords:
Adaptability
COVID-19
NO_2
Socioeconomic recovery
Spatial composition of production factors

ABSTRACT

The COVID-19 pandemic led to a sharp economic contraction. A comprehensive understanding of the relationship between the spatial composition of production factor (SCPF) and socioeconomic recovery is still missing. Here, we applied the contrasting status of nitrogen dioxide (NO_2) concentrations in cities in central and eastern China as natural laboratories. From the perspective of the spatial composition of land (SCL) and the dependence on the inflow population (DIP), four quantifiable indicators (resilience, impact, sensitivity, recovery speed) were used to analyze the adaptability of SCPF to the epidemic lockdown. The results indicate that appropriate SCPF is a prerequisite for a complete "land-population-industry" nexus. The built-up area proportion is below 74.38%, with higher adaptability to epidemic shocks. The range of rural built-up proportion conducive to economic recovery is 10.18%-15.18%. The proportions of various land types inside the city's defense unit should also be constrained. Similarly, DIP is advocated to be maintained below 17.5%. For urban-rural fringe areas, the response to epidemic prevention and socioeconomic recovery are rapid. This observation-driven study indicated that COVID-19 is a shocking reminder for policymakers, to improve the socioeconomic recovery ability from the spatial composition of production factor perspective in the post−COVID−19 era.

1. Introduction

The spread of the COVID-19 pandemic has greatly impeded global socioeconomic development (Dong et al., 2020; Huang et al., 2020). Recovering from the COVID-19 epidemic is one of the greatest concerns in the next few years (Liu et al., 2020a; Wu and Lin, 2020). China enacted a lockdown starting on 23 January 2020, effectively slowing the spread of the epidemic (Chinazzi et al., 2020; Tian et al., 2020). COVID-19 regulations were subsequently implemented worldwide (Tian et al., 2020). Strict epidemic control policy temporarily halted public transportation and industrial production. This socioeconomic "shutdown" reduced productivity and led to a sharp economic contraction (Kraemer et al., 2020). How to make the rapid recovery of socioeconomic activities is still a main problem facing the world.

Socioeconomic recovery is a complex process, including population flow and industrial restart (Zhang et al., 2021). Some studies have found that the unreasonable distribution of population and industries under the COVID-19 has affected regional recovery (Tricarico and De Vidovich, 2021). The spatial composition of production factors (SCPF) mainly includes labor, land and capital (Liu et al., 2018), which is a suitable proxy to reflect the "land-population-industry" nexus (Chen and Quan, 2021). The SCPF directly determines the industrial structure (Chen et al., 2018) and population distribution within the region (Vyatkina et al., 2015). High adaptability to major epidemics requires cities to have two characteristics: speedier response to anti-epidemic policies and faster recovery after control. Therefore, what kind of SCPF has greater adaptability to the epidemic is valuable to reveal (Chen et al., 2018; Percy et al., 2019).

Global Nitrogen dioxide (NO_2) concentrations in lockdowns were 18% (13%–23%) lower than in the same period in 2019 (Bauwens et al.,

* Corresponding author.
E-mail address: zhangjianjun_bj@126.com (J. ZHANG).
# First author: Shidong LIU and Jie ZHANG contributed equally to this manuscript, and should be regarded as co-first authors.

https://doi.org/10.1016/j.scs.2022.104061
Received 20 March 2022; Received in revised form 11 July 2022; Accepted 11 July 2022
Available online 13 July 2022

2020; Keller et al., 2021). Daily NO_2 has been reported to show a short-term decline during the epidemic lockdown (Bauwens et al., 2020; Laughner and Cohen, 2019; Liu et al., 2020b). Therefore, with Covid-19 lockdowns end and economic activity resuming, the NO_2 levels rebound is a typical feature for this time of day (Beirle et al., 2011; Beirle et al., 2019). The atmospheric NO_2 is a suitable indicator for socioeconomic recovery in the region with high temporal and spatial resolution.

In such a turbulent environment, we have questions to ask facing epidemic outbreaks. How does the SCPF affect socioeconomic recovery? What kind of SCPF has the highest adaptability to the epidemic? In the post-epidemic era, how to answer these questions not only puts forward higher requirements for researchers related to urban planning, urban governance and sustainable development around the world, but also brings new challenges to the decision-making of planners and policy-makers. Therefore, in this analysis, we utilized contrasting conditions before and after the COVID-19 outbreak, serving as natural laboratories. Satellite NO_2 measurements were used to monitor central and eastern China (Huang and Sun, 2020). We choose the cell of 35 km^2, average built-up areas in county-level administrative units of China, as the grid unit to analyze the NO_2 change characteristics of different SCPF (Zhou et al., 2012). Four evaluation indicators (resilience, impact, sensitivity, recovery speed) were used to analyze the adaptability of SCPF to the epidemic lockdown. In addition, this study evaluated the relationship between the land-population-industry nexus and the recovery of social activities from the epidemic, combining the dependence on the inflow population (DIP) of industries. Specifically, the objectives of this study were: 1) Quantify the impact of SCPFs on socioeconomic recovery from the COVID-9 epidemic; 2) Identify the range of SCPF corresponding to the maximum adaptability. The results of this study provided specific suggestions on how to improve adaptability to the shock of an epidemic and recovery speed from the four aspects (resilience, impact, sensitivity, and recovery speed). In addition, this study also provides theoretical support and planning basis for epidemic prevention and sustainable development in other countries.

2. Literature review

In the sustainable cities research area after the COVID−19 epidemic, most existing studies focused on socioeconomic recovery. The limited access to bottom-up socioeconomic status and incomplete information related to the industry make it difficult to obtain quantitative estimates of the recovery from the shock of the epidemic. The indicators currently used to reflect socioeconomic recovery mainly involve three aspects: GDP (Shan et al., 2018), population movement (Salvati, 2020), and air pollutant concentration (Zheng et al., 2020). However, socioeconomic indicators such as GDP and population movement are highly dependent on the statistical cycle and cannot reflect daily changes in GDP. Some studies have paid attention to the impact of lockdown on pollutants (Ebenstein et al., 2015; Tollefson, 2020). Notably, NO_2 is predominantly emitted during fossil fuel usage in human activity, related to transportation and industrial production (Seinfeld and Pandis, 2006). NO_2 atmospheric levels showed lower values during holidays (Tan et al., 2009), indicating the close link between NO_2 and human activities. Besides, the lifetime of NO_2 in the atmosphere is relatively short. Thus, atmospheric NO_2 can reflect local changes in economic activities (Atkinson et al., 2018; Lamsal et al., 2011; Seinfeld and Pandis, 2006).

How to promote the recovery in the post−COVID−19 by optimizing the urban structure and function has received more and more attention (Davila et al., 2021; McCartney et al., 2021; Pan et al., 2021). These studies provided suggestions for the recovery of a single industry, such as service (Pan et al., 2021), transportation (Junior et al., 2021; Parker et al., 2021), rural areas (Yu et al., 2021), and industry (Davila et al., 2021; McCartney et al., 2021). However, the overall recovery of the "land-population-industry" nexus still received less attention.

3. Materials and methods

3.1. Study framework

The existing theories regarding the relationships between NO_2 concentration and urban characteristics have been substantiated. Multivariate regression models including urban characteristics explained 54%, 49%, and 37% of the change in NO_2 for large, medium and small cities, respectively (Larkin et al., 2016). Simultaneously, NO_2 concentrations are sensitive to changes in socioeconomic activity intensity due to COVID19 (Dacre et al., 2020). Urban characteristics, population, and land use mixing significantly affect urban NO_2 emissions (Lamsal et al., 2013; Lee, 2019). These studies provide a theoretical basis for our work to identify the impact of SCPF on socioeconomic recovery in the post-epidemic era.

Socioeconomic activities mainly include population activities and industrial operations (Fig. 1a). The SCPF in this study mainly consists of two parts: the spatial composition of land (SCL), and the DIP. The industry structure is directly related to the proportion of land that has become the consensus (Deng et al., 2015). The population is positively correlated with the area of urban and rural residential areas. Commuters driving the regular operation of industries include residents and the inflow population. The lockdown restricted the population mobility, which forced the industry to suspend production (Fig. 1b). This means that recovery is first to lift restrictions on population mobility, and then gradually drive industrial recovery (Fig. 1c). However, it is impossible to open up cross-regional population flow until the epidemic is fully controlled. The matching degree of the population and industry directly affects the socioeconomic recovery. Under a certain SCPF, the matching degree between the people and industry has a significant impact on socioeconomic recovery. In socioeconomic recovery, the SCL may have played a decisive role. This study explored the best SCPF by analyzing the relationship between the SCL, DIP and socioeconomic recovery (troposphere NO_2 column density) in each cell.

3.2. Study area and data set

Central and eastern China are densely populated and relatively developed economies. The epidemic hampered socioeconomic development in this region. However, troposphere NO_2 column density returned to normal levels on March 8, 2020 (Fig. 2). The rapid recovery can provide a reference for other countries. Therefore, this study takes central and eastern China as the study area. According to the NO_2 changes, this study focuses on the daily socioeconomic recovery from January 8 to April 7, 2020 (Liu et al., 2020b; Observatory, 2020).

The data used in this study includes three categories: SCL, DIP, and socioeconomic activities. Landsat data (https://www.usgs.gov/) for 2020, OSM data (https://www.openstreetmap.org/), POI data for 2020 (https://www.resdc.cn/), and essential urban land use categories in China (EULUC-China (Gong et al., 2020) are used to extract the SCL. The population migration data of Baidu Maps (https://map.baidu.com/) for 2020 is used to calculate the DIP. Total population data for each region are obtained from provincial statistical yearbooks (http://www.stats.gov.cn/english/). Daily NO2 data based on TROPOMI Level 2 of Sentinel 5P (Veefkind et al., 2012) and OMI satellite (Lamsal et al., 2011; Levelt et al., 2018) are used to reflect socioeconomic activities. The version 4.0 NASA OMI standard NO2 products (Krotkov, 2016) was used to assist the pre-study in setting the study period (Fig. 2). The version 1.0.0 TROPOMI Level 2 offline NO2 data products for 2019 and the version 1.1.0 data for 2020 (Van Geffen et al., 2020) are used to extract the socioeconomic recovery in each cell. All satellite data used in this study are publicly available through ESA Sentinel-5P Pre-Operations Data Hub (https://s5phub.copernicus.eu/) and NASA Goddard Earth Sciences Data and Information Services Center (https://disc.gsfc.nasa.gov/).

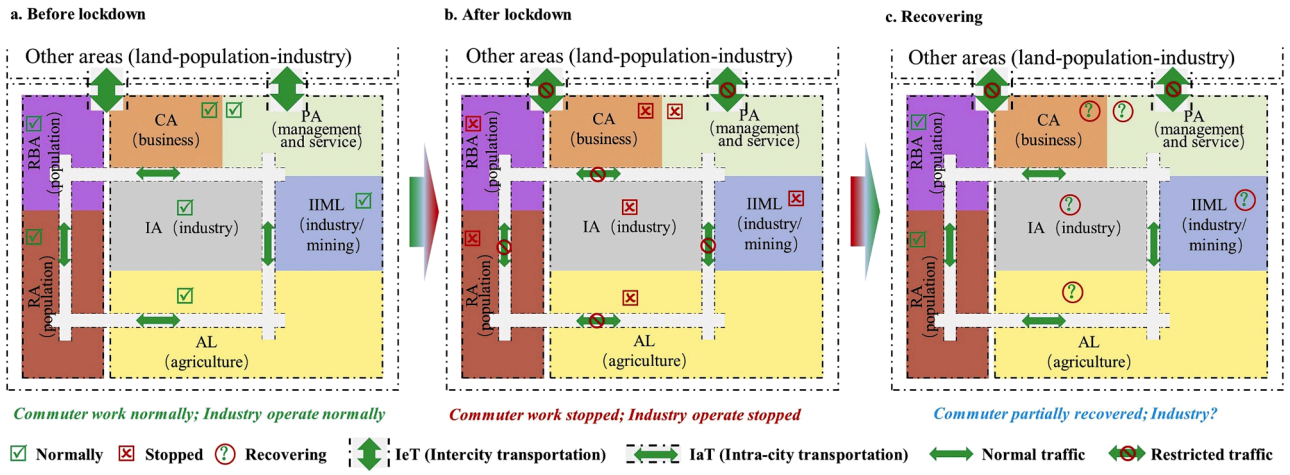

Fig. 1. Study framework. RA: residential area; CA: commercial area; PA: public management and service area; IA: industrial area; IeT: intercity transportation; IaT: intra-city transportation; RBA: rural built-up area; IIML: independent industrial and mining land; AL: agricultural land.

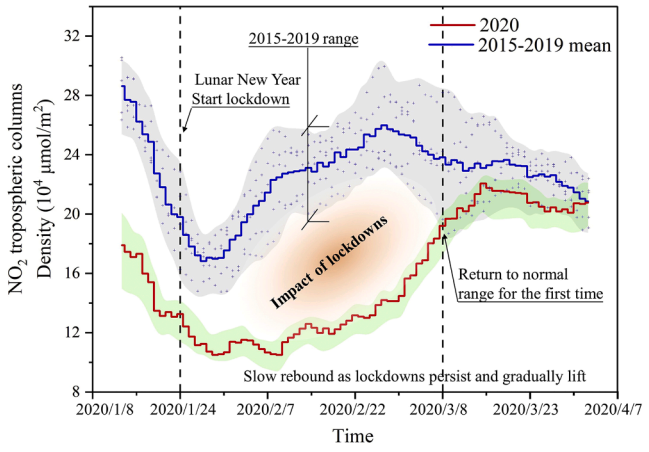

Fig. 2. Daily variations in 7-day moving averages of OMI NO_2 TVCDs over China. Points are plotted at the midpoint of the 7-day moving average.

3.3. Extraction of SCL and DIP

Landsat image is used to distinguish water body, arable land, forest, grassland, and impervious surface through the Supervised Classification of Google Earth Engine (GEE). Arable land, waterbody, forests and grassland are considered to be related to agriculture. The impervious surface is considered to be related to other industries and population settlements. To obtain SCL, OSM road data is used to segment impervious surfaces. At the same time, point of information (POI) and EULUC-China data are used to identify the attributes of each impervious patch after segmentation. Finally, the land in the study area was divided into 9 land types, representing 9 different industries or population distributions (Table S1).

In addition, the population movement data of Baidu Maps is used to analyze the DIP defined by the ratio of the inflow population to the total population. To more clearly reflect the adaptability of the SCPF to the epidemic, SCL and DIP are divided into 5 levels respectively. We define cells without impervious surfaces as inhuman areas (L1). According to the proportion of each land type, other cells are also divided into 4 levels (L2-L5) using the natural breakpoint method. Similarly, the DIP is also divided into 5 levels (LP1-LP5, Table S2).

3.4. Conversion of NO_2 changes to characteristics of socioeconomic recovery

We calculated the NO_2 tropospheric column change between 2019 and 2020 during the study period to explore the spatial aggregation caused by the epidemic lockdown. To reveal the relationship between spatial aggregation of NO_2 change and SCPF, this study exploratorily divided the cities into big-city, mid-city, and small-city based on the proportion of built-up area, and into high DIP (HDIP), medium DIP (MDIP), and low DIP (LDIP) based on the DIP.

Based on the NO_2 data of Sentinel 5P, this study calculates the daily NO_2 fluctuation in each grid in 2019 and 2020. To eliminate the influence of seasonal changes and holidays, this study calculated the ratio of NO_2 in 2020 and 2019 (Liu et al., 2020a), and defined this ratio as the system stability (Percy et al., 2019) of the "land-population-industry" nexus (Fig. 3). This study set a 5% fluctuation as the normal fluctuation range. Since the fluctuation of NO_2 in a single cell is not apparent, we have drawn the change curve of the total amount of NO_2 in each level according to the same land level or DIP level. Based on the system stability curve, some important concepts are defined, such as resilience, impact, sensitivity, and recovery speed (Holling, 1973). The comprehensive performance of these four indicators reflects the region's adaptability to the epidemic lockdown and recovery characteristics. Based on the time-series images of NO_2 concentration, the calculation process of the four indicators reflecting socioeconomic activities' changes characteristics is described in Section 3.5.

Socioeconomic recovery is a complex process, including population

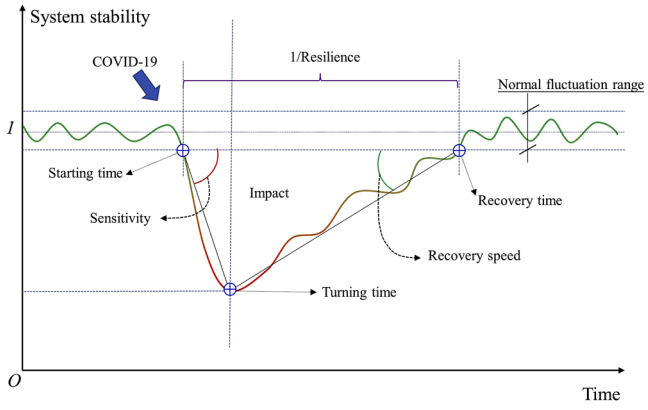

Fig. 3. Concept of evaluation indicators.

flow and industrial restart (Zhang et al., 2021). The unreasonable population distribution and industries under the COVID-19 has affected regional recovery (Tricarico and De Vidovich, 2021). The proportion of land can be used to reflect the location and spatial accumulation of industrial distribution (Deng et al., 2015). As two important indicators representing SCPFs, SCL demonstrates the state of land use and industry in the region, and DIP reflects the population flow in the region.

By comparing the recovery situation with different SCPFs, we define the areas with high adaptability as the best areas, and determine the corresponding SCLs as the optimal SCLs. Similarly, the optimal DIP is also defined. Finally, by searching for the proportions of land and the proportion of inflow populations corresponding to different land levels and DIP levels, this study quantified the optimal SCPF, including optimal SCL and the optimal DIP.

3.5. Extraction of socioeconomic activities change

To extract the change characteristics of socioeconomic activities from the time series of NO_2 concentration, we build a maximum disturbance identification model (MDIM). The model calculates the system's sensitivity, resilience, recovery speed, and impact (Fig. 3) by identifying the location, degree, change point, and duration in different phases of the largest disturbance.

Step 1: Noise cancellation. X_{ijz} is the NO_2 concentration of row i, column j, and day z. By the 7-day moving average of NO_2 (Eq. (1)), the clean NO_2 time series image ($\overline{X_{ijz}}$) is calculated.

$$\overline{X_{ijz}} = \frac{1}{7}\sum_{z-3}^{z+3} X_{ijz} \tag{1}$$

Step 2: System stability calculation. According to the definition in Section 3.4, the system stability indicator (S_{ijz}) is calculated based on the clean NO_2 time series images in 2019 ($\overline{X_{ijz}}_{2019}$) and 2020 ($\overline{X_{ijz}}_{2020}$).

$$S_{ijz} = \frac{\overline{X_{ijz}}_{2020}}{\overline{X_{ijz}}_{2019}} \tag{2}$$

Step 3: Binarization. To simplify the identification process, the simplified series (O_{ijz}) is calculated by the binarization method. Here, a value less than 1 is considered a value disturbed by the epidemic.

$$O_{ijz} = IF\left(S_{ijz} \le 1,\ 1,\ 0\right) \tag{3}$$

Step 4: Longest continuous disturbance days calculation. We first calculate the length of continuous disturbance days (L_{ijz}) continuously affected by the epidemic lockdown through the recursive formula based on the binarized result (O_{ijz}). Then, the longest continuous disturbance days (N_{max}) is obtained by finding the maximum value.

$$L_{ijz} = \begin{cases} 0 & z = 0 \\ O_{ijz} \times \left(O_{ijz} + L_{ijz-1}\right) & z > 0 \end{cases} \tag{4}$$

$$N_{max} = Max\left(L_{ijz}\right) \tag{5}$$

Step 5: Determination of start and recovery moments of the disturbance. The recovery time (T_e) corresponding to the longest continuous disturbance is found by finding the position of (N_{max}) in (L_{ijz}). Then, the start time (T_s) is calculated from (N_{max}).

$$T_e = Find\left(L_{ijz} = N_{max}\right) \tag{6}$$

$$T_s = T_e - N_{max} \tag{7}$$

Step 6: Determination of trend change point. The epidemic lockdown caused the NO_2 concentration to decrease gradually, and then increase gradually after control. Therefore, the time corresponding to the minimum value of S_{ijz} is recorded as the change point (T_c).

$$T_c = Find\left(S_{ijz} = Min\left(S_{ijz}\right)\right) \tag{8}$$

Step 7: Sensitivity and recovery speed calculations. According to the definition in Section 3.4, the sensitivity and recovery speed within the region is calculated by calculating the decline speed and recovery speed of the system stability curve.

$$Sensitivity_{ij} = \frac{1 - Min\left(S_{ijz}\right)}{T_c - T_s} \tag{9}$$

$$Recovery\_speed_{ij} = \frac{1 - Min\left(S_{ijz}\right)}{T_e - T_c} \tag{10}$$

Step 8: Resilience calculation. According to the definition in Section 3.4, the region with a longer disturbance time has poorer resilience. Resilience is inversely proportional to the longest continuous disturbance days.

$$Resilience_{ij} = \frac{1}{N_{max}} \tag{11}$$

Step 9: Impact calculation. The impact is calculated by calculating the area of the downward fluctuation of the system stability curve during the disturbance.

$$Impact_{ij} = \sum_{T_s}^{T_e} S_{ijz} \approx \frac{1}{2} \times N_{max} \times \left(1 - Min\left(S_{ijz}\right)\right) \tag{12}$$

4. Results and analysis

4.1. Spatiotemporal differentiation of NO_2 changes

The changes in the NO_2 tropospheric column caused by the epidemic lockdown have spatial agglomeration (Fig. 4a). The decline of socioeconomic activity is mainly concentrated in the built-up areas of large cities, such as Beijing, Guangzhou, Wuhan, and Zhengzhou. However, there are some cities where the NO_2 decline is not apparent, such as Hangzhou and Nanjing.

The role of rural built-up areas in resisting the impact of the epidemic is obvious in a larger city (Fig. 4b). In large cities, the greater proportion difference between urban and rural with the less obvious NO_2 density decrease ($R=0.78$, $P<0.05$). In mid- and small-cities, this change is the opposite (mid-: $R=-0.06$, $P>0.05$; small-: $R=-0.25$, $P<0.05$). From the perspective of DIP (Fig. 4c), there is a positive correlation between proportion difference and changes in NO_2 in HDIP ($R=0.19$, $P>0.05$). In MDIP and LDIP, this trend is opposite (MDIP: $R=-0.14$, $P>0.05$; LDIP: $R=-0.22$, $P<0.05$). The result reflects that the scale, composition of built-up area and DIP related to different adaptability to the epidemic.

4.2. The adaptability of socioeconomic to the shock of epidemic

4.2.1. Impact of SCL on adaptability to the epidemic

The adaptability of different SCLs to the epidemic varies greatly. Larger built-up areas have less resilience and slower recovery speed,

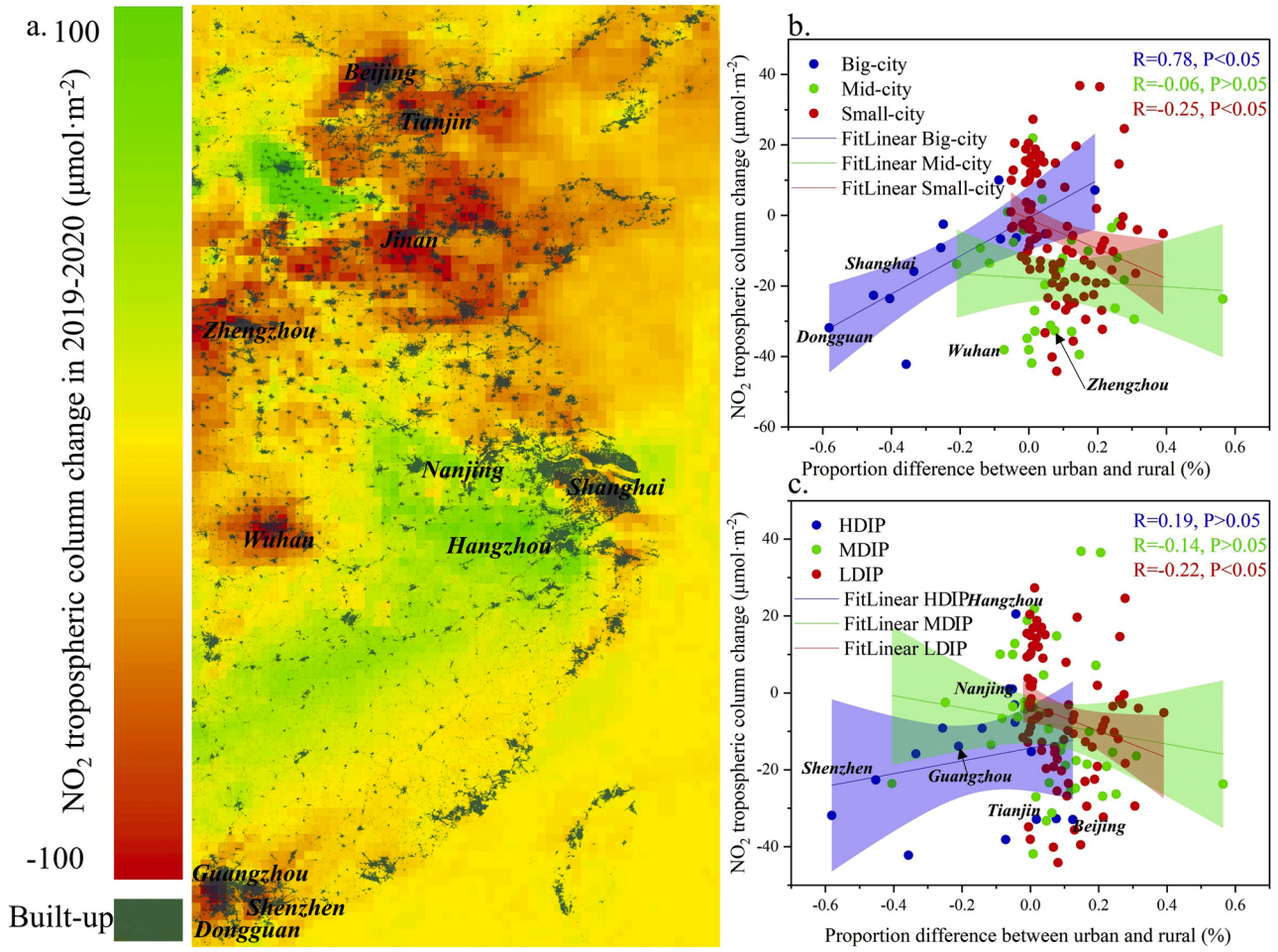

Fig. 4. Proportion of NO_2 concentration change between 2019 and 2020. **b** is the result of statistics based on the size of the city; **c** is the result of statistics based on the difference between urban-rural structures; Proportion difference between urban and rural is the result of subtracting the proportion of urban built-up area from the proportion of the rural built-up area.

which amplified the impact of the epidemic on socioeconomic. The total scale of the built-up area is best controlled below L4. Within the built-up area, the smaller the residential area and commercial area, the greater the resilience and the smaller the impact. Appropriately reducing the proportion of the residential area is conductive to improve recovery speed. Although the reduction in the commercial area reduces the response speed, this reduction is weak. Therefore, the proportion of residential area and the commercial area should be controlled below L3 and L4, respectively. Smaller public management and service area has greater resilience, response and recovery speed. The medium public management and service area has the slowest recovery rate, which makes the impact of the epidemic lockdowns even greater. Therefore, it is necessary to maintain a small public management and service area (less than L3). The larger the industrial area, the smaller the resilience and recovery speed, and the greater the impact. When the industrial area exceeds L2, the response speed decreases significantly (a decrease of more than 72.73%).

The increase in the proportion of intercity transportation and intra-city transportation reduces the resilience and increases the impact of the epidemic lockdowns. Larger transportation land reduces the response and recovery speed. Intercity transportation and intra-city transportation are best controlled within L4 and L3 respectively. When the intercity traffic is at L3, the adaptability of the area is greatest, which may be related to the inflow population. A larger rural built-up area has a greater resilience and recovery speed. But when the rural built-up area exceeds L4, the impact of the epidemic lockdowns will increase. Since the rural built-up area has the slowest response speed at L3, the rural built-up area should be better controlled at L4. When the proportion of independent industrial and mining land is less than L3, the resilience is greater and the impact of the epidemic lockdowns is minimal. Appropriate reduction of independent industrial and mining land can effectively improve response and recovery speed.

4.2.2. *Impact of DIP on adaptability to the epidemic*

The recovery from the epidemic lockdown largely depends on the return of commuters. In addition to SCL, the socioeconomic recovery is related to the DIP (Fig. 6). The recovery of regions with high DIPs is more affected by cross-regional population movement. The regions highly dependent on the local population have the opposite situation. The higher the DIP, the smaller the resilience (Fig. 6a) and the slower the recovery speed (Fig. 6d). In addition, the impact of the epidemic lockdown intensified with the DIP increases (Fig. 6b). When DIP is in LP1 and LP5, the response speed is the fastest (Fig. 6c). Therefore, DIP is necessary to control below LP1.

Appropriate reduction of regional DIP is conducive to adaptability. Reducing DIP requires optimizing the regional industrial structure, which indicates a suitable land layout. Rationally adjusting the supply and structure of various land, such as maintaining a certain amount of rural built-up area, reducing commercial area and public management and service area, and transforming the industrial area, has an obvious effect on the socioeconomic recovery.

4.2.3. Optimal SCPF for socioeconomic recovering from epidemic

Based on weighing the four indicators (Fig. 5; Fig. 6), the optimal SCPF is formed (Table 1). When the total built-up area needs to be maintained at less than 74.38%, the impact in this region is low, and the resilience, response and recovery speed are high. The normal circulation between regional people and industry requires a complete industrial structure and reasonable SCL. As an indispensable part, rural built-up areas should also be kept between 10.18%-15.18%. Similarly, DIP needs to be maintained at less than 17.5%. It can ensure that the population of the region is sufficient to support the industrial recovery when the cross-regional population flow is restricted.

4.3. Socioeconomic recovery process and adaptability performance in different areas

To verify the optimal SCL and DIP, this study calculated the score (0-10) of each area, the number of indicators that meet the optimal SCPF. According to the score, all areas are divided into 4 categories: inhuman area, no adaptability (0-3), low adaptability (4-7), and high adaptability (8-10). There are spatial differences in the adaptability of different regions to the epidemic (Fig. 7a). High adaptive areas are distributed in urban-rural fringe areas and small cities with complete urban functions and small DIP. Low adaptive areas are distributed in urban-rural fringe areas and small cities with incomplete urban functions. Maladaptive areas are distributed in urban dominated areas (No adaptability U) and rural dominated areas (No adaptability R). From the time perspective, the recovery of urban, rural, and inhuman areas mainly occurs during the main recovery interval (January 21 to March 7). Still, the recovery situation is significantly different (Fig. 7b). During the main recovery interval, the high adaptability area returns to the normal level the fastest, and the response to implementing epidemic prevention measures and policies is the fastest (Fig. 7c). Although the epidemic prevention measures have had a significant impact on socioeconomic activities in a short period, the region can achieve rapid recovery when the epidemic is under control.

In the three phases of socioeconomic recovery, our evaluation results have been verified. The division of the three recovery phases is based on the volatility characteristics of the curve. In addition, we have found the actual policy or report basis corresponding to these recoveries and suspension (Table S3). Except for the start recovery phase, which only considered special enterprises such as medical supplies manufacturers, the high-adaptability areas in the subsequent two recoveries showed

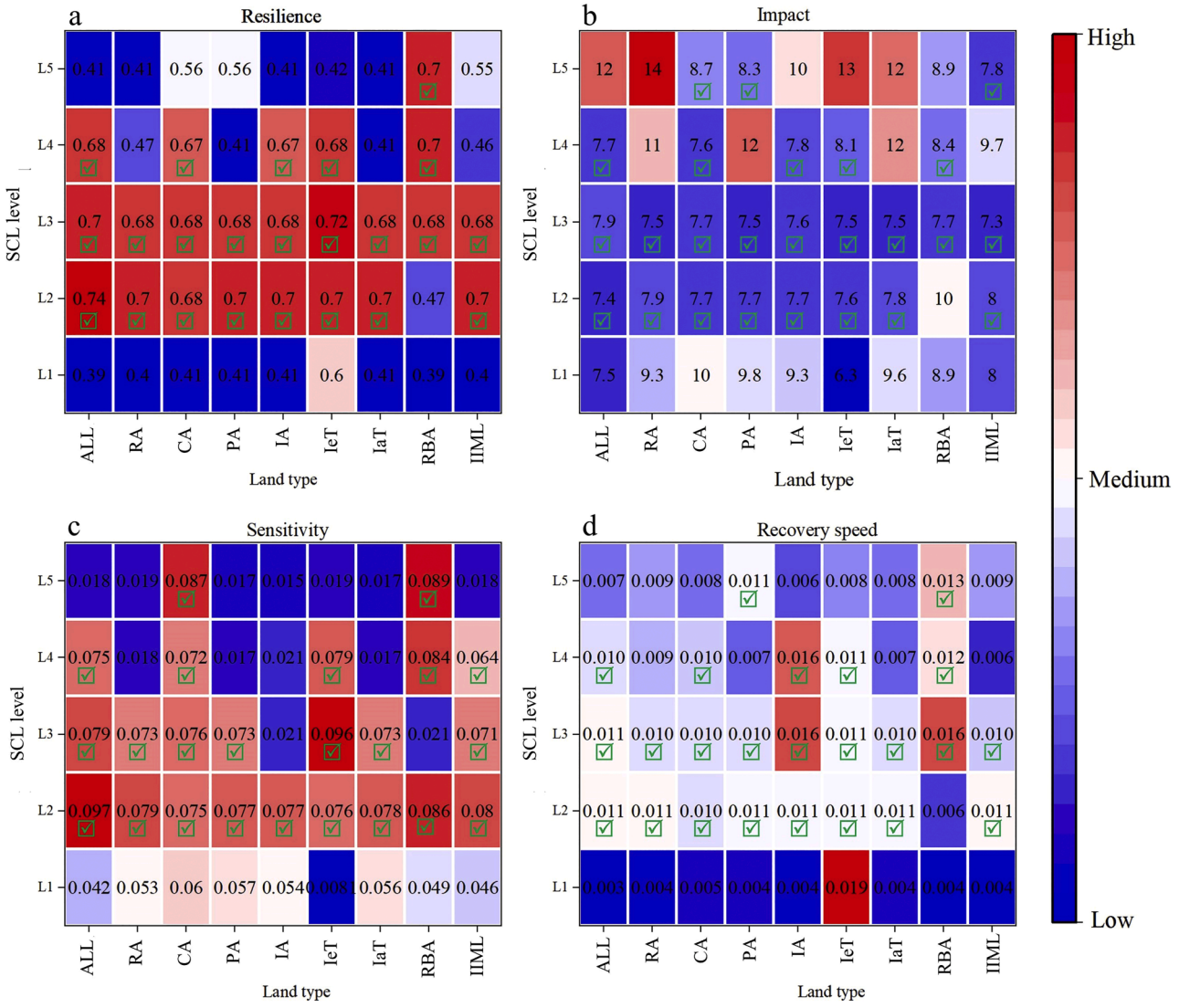

Fig. 5. Impact of SCL on adaptability to the epidemic. ALL: total built-up; RA: residential area; CA: commercial area; PA: public management and service area; IA: industrial area; IeT: intercity transportation; IaT: intra-city transportation; BRA: rural built-up area; IIML: independent industrial and mining land. L1 is mainly an inhuman area; the "☑" represents that the SCL level is better than the average in terms of adaptability to the epidemic.

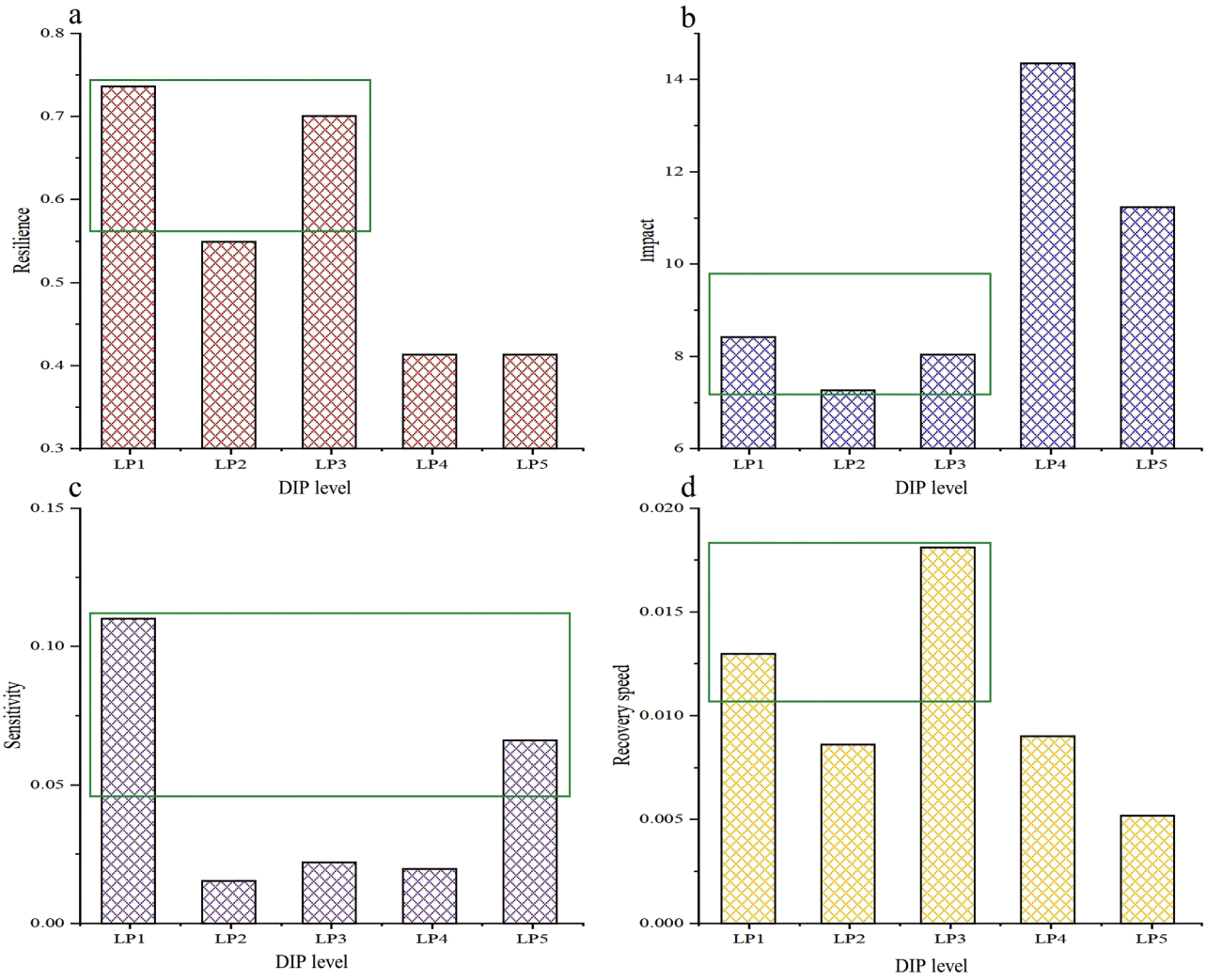

Fig. 6. Impact of DIP on adaptability to the epidemic. The green box represents that the DIP level is better than the average in terms of adaptability to the epidemic.

Table 1
Optimal SCPF for greater adaptability.

SCPF		Comprehensive optimal level	
		Optimal level	Actual range (%)
SCL	All	<L4	<74.38
	RA	<L3	<12.77
	CA	<L4	<7.79
	PA	<L3	<4.59
	IA	<L2	<5.16
	IeT	<L4	<2.13
	IaT	<L3	<1.96
	RBA	=L4	10.18 - 15.18
	IIML	<L3	<2.7
DIP		<LP1	<17.5

Note: SCPF: spatial composition of production factor; SCL: spatial composition of land; DIP: dependence on the inflow population.

strong adaptability (Fig. 7c). Both the policy response speed and the socioeconomic recovery speed has eased and show regular characteristics: high adaptability area> low adaptability area> average state> no adaptability area in rural> no adaptability area in urban.

5. Discussion

5.1. Implications for socioeconomic recovery and sustainable cities

The socioeconomic recovery after the COVID-19 pandemic is an essential indicator of sustainable cities. Quantification of the optimal range of SCPF provides a scientific base to support socioeconomic recovery and sustainable cities and society. According to our results, proper adjustment of urban-rural structure is a crucial way to promote rapid socio-economic recovery. For the epidemic lockdown, appropriate SCL and DIP are conducive to improving the adaptability of the region. Adaptation to major emergencies should also be included in the concept of sustainable cities. The larger the city, the more vital the role of rural built-up areas in resisting the impact of the epidemic lockdown. Therefore, in urbanization, retaining some rural areas with perfect infrastructure can provide basic conditions for socioeconomic recovery after reopening, such as produce and laborers. Furthermore, policymakers should pay attention to the vital role played by the urban-rural fringe in the process of socioeconomic recovery. DIP is smaller for the recovery in the rural-urban fringe. Not only the response to epidemic prevention measures and policies is sensitive here, but also the socioeconomic recovery is rapid when the COVID-19 is under control. However, it is necessary to ensure that the SCPF at the urban-rural fringe areas is appropriate, thereby ensuring the integrity of urban functions. The coordinated "land-population-industry" nexus is the prerequisite for

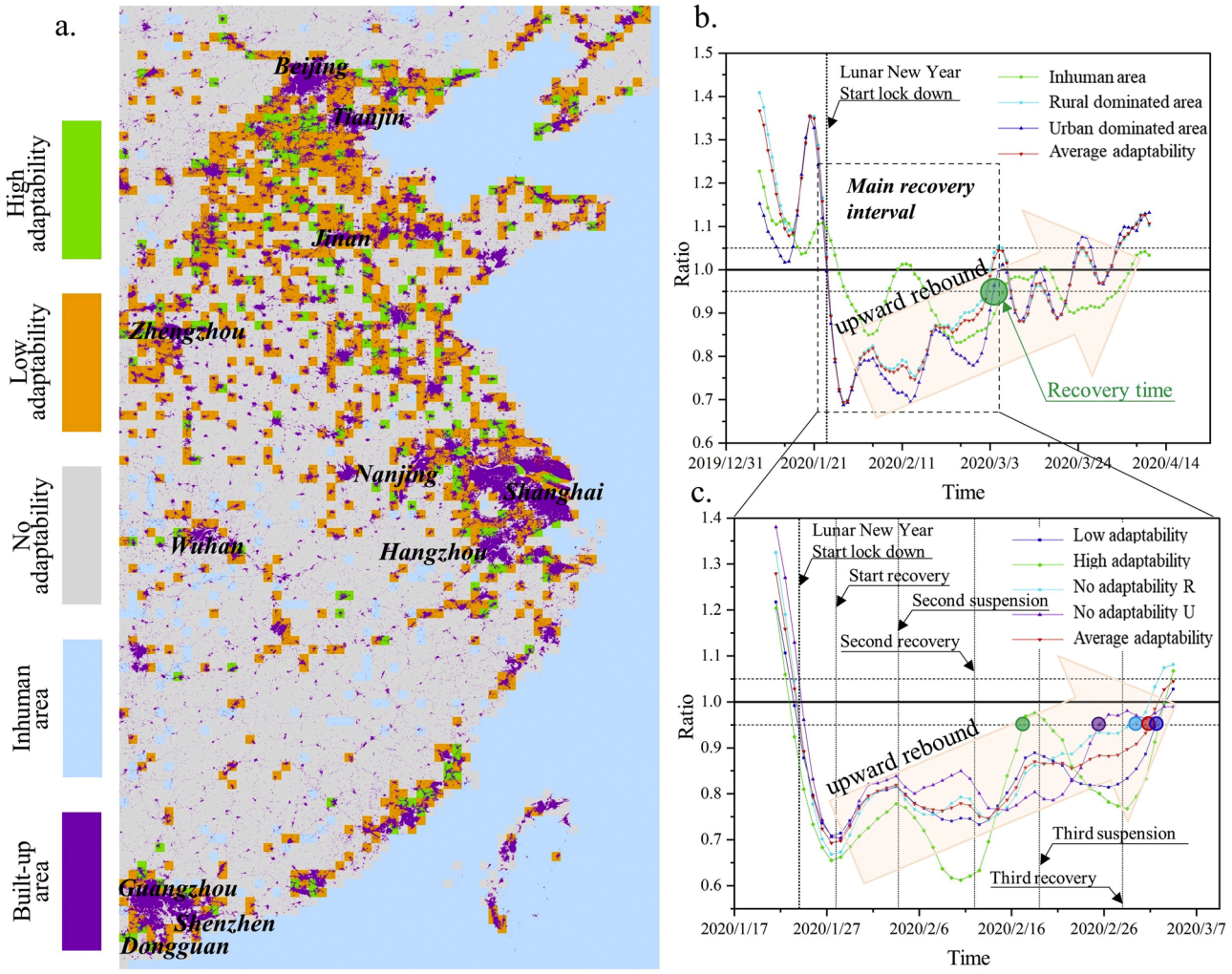

Fig. 7. Spatial distribution and adaptability performance in different areas. The **a.** is the spatial distribution of different adaptability areas. The **b.** reflects the main interval of the epidemic recovery. The **c.** reflects the recovery performance of different adaptability areas in different phases.

driving the rapid recovery and improving urban sustainability within the city.

The sustainability of a city is inseparable from the perfect cooperation between industry and laborers. The industry recovery is inseparable from the return of laborers. In the absence of cross-regional commuting, the unreasonable industrial structure leads to laborers being unable to work. This mismatch means that the lower the DIP, the faster the supply of laborers for the socioeconomic recovery. Similarly, industries with higher DIPs have slower recovery speeds. Appropriate residential areas and rural built-up areas are necessary to host the local population. On the contrary, uncoordinated "land-population-industry" nexus amplified the impact of the epidemic, thus hampering social and economic recovery. Although the Chinese government issued policies to promote cross-regional workers staying at the workplace during the spring festival of 2020 (China, 2021), this is only an expedient measure. A reasonable supply of local workers and industrial structure are the basic needs for rapid recovery under the epidemic lockdown. Therefore, adjustment of SCPF is an important way to coordinate the "land--population-industry" nexus.

5.2. *Implications for sustainable planning and policy in the post-epidemic era*

This study provided a sustainable planning and policy basis and recommendations for other countries by analyzing China's recovery experience. When there is no epidemic situation, cities generally set the SCPF based on socioeconomic development. Once the epidemic outbreak, it is difficult to adjust the SCPF temporarily. Land use planning, urban planning, urban-rural planning, and industrial planning have been developed (Liu and Zhou, 2021; Zhou et al., 2017). However, the shortcomings of the current planning have been fully exposed under the COVID-19 epidemic: lack of adaptability to the shock of epidemics. Therefore, the land structure needs to be adjusted. Solving these shortcomings requires planners and policymakers to consider the adaptability and sustainability of cities when formulating plans and policies, such as retaining some land that can be temporarily adjusted. Spatial planning already contains the most important and latest concept of territorial spatial planning in China (Liu and Zhou, 2021). Under the requirements of improved adaptability and sustainability, our result highlights the concept of defense unit: an area with reasonable SCPF to coordinate the "land-population-industry" nexus. Establishing defense units with high adaptability to the shock of epidemic helped to target measures for economic recovery in the post−COVID−19 era. Although the total built-up area, rural built-up area and independent industrial and mining land are not within the urban built-up areas, they played an essential role in the socioeconomic recovery from the epidemic lockdown. The proportion of these land types within the cell should also be considered. Coordinating the SCPF in the defense unit is the basis for improving the adaptability of the "land-population-industry" nexus.

If the urban industry and scale expand disorderly, the urban "land-

population-industry" nexus will become unsustainable. To reduce the impact of the epidemic lockdown, we suggest appropriately cutting out non-essential functions in big cities, and developing policies for urban renewal. It is worth noting that the public management and service area is an indispensable part of maintaining the normal operation of the city. For epidemic lockdown, especially hospital land, public management and service area are important indicators for improving urban epidemic control capabilities and socioeconomic recovery. Therefore, we recommend increasing the proportion of public management and service area.

This study also supports the view that rural built-up area has an indispensable role in fighting the epidemic (Wang and Zhao, 2020). Therefore, policymakers should also emphasize the complete functions of urban-rural fringe zones and small cities. To promote the urban-rural integration development and make up for regional shortcomings, managers should provide support from land supply and spatial layout. Furthermore, the urban-rural fringe zone can provide a large number of workers and food for socioeconomic recovery. Therefore, the stability and adaptability of the urban-rural fringe are directly related to sustainable cities and society. It is essential to formulate a reasonable rural revitalization strategy and new rural countryside policy.

5.3. Limitations and uncertainties

This study extracted indicators of socioeconomic recovery based on 2019 and 2020 data. Except for the epidemic lockdown, the difference in NO_2 between the adjacent two years is little. Therefore, we assumed that the NO_2 concentration in 2020 before the epidemic lockdown and after the recovery is equivalent to 2019. Furthermore, we assume there will be no cross-regional population flow until the epidemic is fully controlled. Although there may be a small flow, such as medical and material aid workers, we consider this to have a negligible impact on atmospheric NO_2. We exploratorily used $35km^2$ as a defense unit. Perhaps it is more reasonable to dynamically adjust the size of the defense unit according to the characteristics of different areas. In contrast, the size of the defense unit is needed to be discussed in further study.

6. Conclusions

The core finding of this study is that the evolution of NO2 varies from one urban characteristic to another, therefore SCPF plays a non-ignorable role in socioeconomic recovery from an impact, resilience, sensitivity, and recovery speed perspective. For the COVID-19 epidemic lockdown, SCL and DIP have a great impact on regional adaptability. The larger the city, the more vital the role of rural built-up areas in resisting the impact of the epidemic lockdown. The urban-rural fringe is not only very sensitive to the epidemic prevention measures and policies, but also the socioeconomic recovery is rapid when the COVID-19 is under control. However, it is necessary to ensure that the SCPF at the urban-rural fringe areas is appropriate. The formation of a complete "land-population-industry" nexus is the prerequisite for driving the rapid recovery within the city.

The contribution of this study is to quantify the optimal range of SCPF, which provides scientific bases to support socioeconomic recovery. The higher adaptability of the region requires the proportions of total built-up area to be controlled below 74.38%. The proportions of various land types inside the defense unit should also be constrained. As an indispensable part, the rural built-up area should also be kept between 10.18%-15.18%. Similarly, DIP needs to be maintained at less than 17.5%.

Declaration of Competing Interest

The authors declared that they have no conflicts of interest to this work. We declare that we do not have any commercial or associative interest that represents a conflict of interest in connection with the work submitted.

Data Availability

We have shared the link of the data source in the article.

Acknowledgment

This work was supported by National Key R&D Program of China (Grant No: 2019YFC0507804), the Fundamental Research Funds for the Central Universities (Grant No: 2652018033) and State Scholarship Fund of China Scholarship Council (Grant No: 202106400019).

Supplementary materials

Supplementary material associated with this article can be found, in the online version, at doi:10.1016/j.scs.2022.104061.

References

Atkinson, R. W., Butland, B. K., Anderson, H. R., & Maynard, R. L. (2018). Long-term concentrations of nitrogen dioxide and mortality: a meta-analysis of cohort studies. *Epidemiology (Cambridge, Mass.), 29*(4), 460.

Bauwens, M. et al., 2020. Impact of coronavirus outbreak on NO2 pollution assessed using TROPOMI and OMI observations. Geophys. Res. Lett., 2020, e2020GL087978.

Beirle, S., Boersma, K. F., Platt, U., Lawrence, M. G., & Wagner, T. (2011). Megacity emissions and lifetimes of nitrogen oxides probed from space. *Science, 333*(6050), 1737–1739.

Beirle, S., et al. (2019). Pinpointing nitrogen oxide emissions from space. *Science advances, 5*(11). eaax9800.

Chen, W., Shen, Y., & Wang, Y. (2018). Does industrial land price lead to industrial diffusion in China? An empirical study from a spatial perspective. *Sustainable cities and society, 40*, 307–316.

Chen, X., & Quan, R. (2021). A spatiotemporal analysis of urban resilience to the COVID-19 pandemic in the Yangtze River Delta. *Nat. Hazards, 106*(1), 829–854.

China, G.O.o.t.S.C.o.t.P.s.R.o., 2021. Notice on Doing a Good Job in Relevant Work during the New Year's Day and Spring Festival in 2021.

Chinazzi, M., et al. (2020). The effect of travel restrictions on the spread of the 2019 novel coronavirus (COVID-19) outbreak. *Science, 368*(6489), 395–400.

Dacre, H. F., Mortimer, A. H., & Neal, L. S. (2020). How have surface NO2 concentrations changed as a result of the UK's COVID-19 travel restrictions? *Environ. Res. Lett, 15*(10).

Davila, F., et al. (2021). COVID-19 and food systems in Pacific Island Countries, Papua New Guinea, and Timor-Leste: Opportunities for actions towards the sustainable development goals. *Agricultural Systems, 191*, Article 103137.

Deng, X., Huang, J., Rozelle, S., Zhang, J., & Li, Z. (2015). Impact of urbanization on cultivated land changes in China. *Land use policy, 45*, 1–7.

Dong, E., Du, H., & Gardner, L. (2020). An interactive web-based dashboard to track COVID-19 in real time. *The Lancet infectious diseases, 20*(5), 533–534.

Ebenstein, A., et al. (2015). Growth, pollution, and life expectancy: China from 1991-2012. *Amer. Econ. Rev., 105*(5), 226–231.

Gong, P., et al. (2020). Mapping essential urban land use categories in China (EULUC-China): Preliminary results for 2018. *Science Bulletin, 65*(3), 182–187.

Holling, C. S. (1973). Resilience and stability of ecological systems. *Annu. Rev. Ecol. Syst., 4*(1), 1–23.

Huang, C., et al. (2020). Clinical features of patients infected with 2019 novel coronavirus in Wuhan. *China. The lancet, 395*(10223), 497–506.

Huang, G., & Sun, K. (2020). Non-negligible impacts of clean air regulations on the reduction of tropospheric NO2 over East China during the COVID-19 pandemic observed by OMI and TROPOMI. *Sci. Tot. Environ., 745*, Article 141023.

Junior, A. A. B., Faria, W. R., Proque, A. L., Perobelli, F. S., & de Almeida Vale, V. (2021). COVID-19, Public Agglomerations and Economic Effects: Assessing the Recovery Time of Passenger Transport Services in Brazil. *Transp. Policy.*

Keller, C. A., et al. (2021). Global impact of COVID-19 restrictions on the surface concentrations of nitrogen dioxide and ozone. *Atmos. Chem. Phys., 21*(5), 3555–3592.

Kraemer, M. U., et al. (2020). The effect of human mobility and control measures on the COVID-19 epidemic in China. *Science, 368*(6490), 493–497.

Krotkov, N., 2016. A. and Veefkind, P.: OMI/Aura Nitrogen Dioxide (NO2) Total and Tropospheric Column 1-orbit L2 Swath 13×24 km V003, Greenbelt, MD, USA, Goddard Earth Sciences Data and Information Services Center (GES DISC).

Lamsal, L., et al. (2011). Application of satellite observations for timely updates to global anthropogenic NOx emission inventories. *Geophys. Res. Lett., 38*(5).

Lamsal, L. N., Martin, R. V., Parrish, D. D., & Krotkov, N. A. (2013). Scaling Relationship for NO2 Pollution and Urban Population Size: A Satellite Perspective. *Environ. Sci. Technol., 47*(14), 7855–7861.

Larkin, A., van Donkelaar, A., Geddes, J. A., Martin, R. V., & Hystad, P. (2016). Relationships between Changes in Urban Characteristics and Air Quality in East Asia from 2000 to 2010. *Environ. Sci. Technol., 50*(17), 9142–9149.

Laughner, J. L., & Cohen, R. C. (2019). Direct observation of changing NOx lifetime in North American cities. *Science, 366*(6466), 723–727.

Lee, C. (2019). Impacts of urban form on air quality in metropolitan areas in the United States. *Computers Environment and Urban Systems*, 77.
Levelt, P. F., et al. (2018). The Ozone Monitoring Instrument: overview of 14 years in space. *Atmos. Chem. Phys., 18*(8), 5699–5745.
Liu, F., et al. (2020a). Abrupt decline in tropospheric nitrogen dioxide over China after the outbreak of COVID-19. *Science Advances, 6*(28). eabc2992.
Liu, F., et al. (2020b). Abrupt decline in tropospheric nitrogen dioxide over China after the outbreak of COVID-19. *Science Advances, 6*(28).
Liu, Y., Zhang, Z., & Zhou, Y. (2018). Efficiency of construction land allocation in China: An econometric analysis of panel data. *Land Use Policy, 74*, 261–272.
Liu, Y., & Zhou, Y. (2021). Territory spatial planning and national governance system in China. *Land Use Policy, 102*, Article 105288.
McCartney, G., Pinto, J., & Liu, M. (2021). City resilience and recovery from COVID-19: The case of Macao. *Cities, 112*, Article 103130.
Observatory, N.E., 2020. Nitrogen Dioxide Levels Rebound in China, pp. 20.
Pan, J., Bardhan, R., & Jin, Y. (2021). Spatial distributive effects of public green space and COVID-19 infection in London. *Urban For. Urban Green., 62*, Article 127182.
Parker, M. E., et al. (2021). Public transit use in the United States in the era of COVID-19: Transit riders' travel behavior in the COVID-19 impact and recovery period. *Transp. Policy, 111*, 53–62.
Percy, D. B., et al. (2019). Mental toughness in surgeons: Is there room for improvement? *Can. J. Surg., 62*(6), 482–487.
Salvati, L. (2020). Residential mobility and the local context: Comparing long-term and short-term spatial trends of population movements in Greece. *Socioecon. Plann. Sci., 72*, Article 100910.
Seinfeld, J.H. and Pandis, S.N., 2006. Atmospheric chemistry and physicsfrom air pollution to climate change.
Shan, Y., et al. (2018). City-level climate change mitigation in China. *Science advances, 4*(6). eaaq0390.
Tan, P.-H., Chou, C., Liang, J.-Y., Chou, C. C.-K., & Shiu, C.-J. (2009). Air pollution "holiday effect" resulting from the Chinese New Year. *Atmos. Environ., 43*(13), 2114–2124.
Tian, H., et al. (2020). An investigation of transmission control measures during the first 50 days of the COVID-19 epidemic in China. *Science, 368*(6491), 638–642.
Tollefson, J. (2020). How the coronavirus pandemic slashed carbon emissions—In five graphs. *Nature, 582*(7811), 158–159.
Tricarico, L., & De Vidovich, L. (2021). Proximity and post-COVID-19 urban development: Reflections from Milan, Italy. *Journal of Urban Management*.
Van Geffen, J., et al. (2020). S5P TROPOMI NO2 slant column retrieval: method, stability, uncertainties and comparisons with OMI. *Atmospheric Measurement Techniques, 13*(3), 1315–1335.
Veefkind, J., et al. (2012). TROPOMI on the ESA Sentinel-5 Precursor: A GMES mission for global observations of the atmospheric composition for climate, air quality and ozone layer applications. *Remote Sens. Environ., 120*, 70–83.
Vyatkina, O. O., Kurilkin, A. V., Mukhina, K. D., Mityagin, S. A., & Boukhanovsky, A. V. (2015). Data-driven modeling of MRT-based population mobility using impersonal data. *Procedia Computer Science, 66*, 356–363.
Wang, Y., & Zhao, Y. (2020). Investigation and Research on Rural Residents' Cognition of COVID-19 and Preventive Measures. *China. Chinese General Practice Nursing, 18*(8), 978–980.
Wu, S., & Lin, M. (2020). Analyzing the Chinese budgetary responses to COVID-19: balancing prevention and control with socioeconomic recovery. *Journal of Public Budgeting, Accounting & Financial Management*.
Yu, X., Zhang, Y. and Sun, H., 2021. Modeling COVID-19 spreading dynamics and unemployment rate evolution in rural and urban counties of Alabama and New York using fractional derivative models. Results in Physics: 104360.
Zhang, J., et al. (2021). The impact of relaxing interventions on human contact patterns and SARS-CoV-2 transmission in China. *Science Advances, 7*(19), eabe2584.
Zheng, B., et al. (2020). Satellite-based estimates of decline and rebound in China's CO2 emissions during COVID-19 pandemic. *Science Advances, 6*(49). eabd4998.
Zhou, W. L., Martinon-Torres, M., Chen, J. L., Liu, H. W., & Li, Y. X. (2012). Distilling zinc for the Ming Dynasty: the technology of large scale zinc production in Fengdu, southwest. *China. J. Archaeol. Sci., 39*(4), 908–921.
Zhou, X., Lu, X., Lian, H., Chen, Y., & Wu, Y. (2017). Construction of a Spatial Planning system at city-level: Case study of "integration of multi-planning" in Yulin City. *China. Habitat International, 65*, 32–48.